

## Article

# A Robust Controller for Upper Limb Rehabilitation Exoskeleton

Andrés Blanco-Ortega , Luis Vázquez-Sánchez , Manuel Adam-Medina, Jorge Colín-Ocampo, Arturo Abúndez-Pliego, Claudia Cortés-García  and Carlos Daniel García-Beltrán

Tecnológico Nacional de México-CENIDET, Cuernavaca 62490, Mexico; andres.bo@cenidet.tecnm.mx (A.B.-O.); manuel.am@cenidet.tecnm.mx (M.A.-M.); jorge.co@cenidet.tecnm.mx (J.C.-O.); arturo.ap@cenidet.tecnm.mx (A.A.-P.); claudia.cg@cenidet.tecnm.mx (C.C.-G.); carlos.gb@cenidet.tecnm.mx (C.D.G.-B.)

\* Correspondence: leviathan11910e@cenidet.edu.mx

**Abstract:** In this paper, a portable exoskeleton for the rehabilitation of upper extremities of three degrees of freedom (DOF) is proposed. With these degrees of freedom, the exoskeleton provides the movements of flexion–extension and abduction–adduction of the arm and flexion–extension of the forearm. A robust generalized proportional integral (GPI) controller for trajectory tracking to provide smooth movements for rehabilitation with the exoskeleton is proposed. This controller only requires output measurements and is robust against different types of disturbances. Simulation results are presented in the MSC Adams® software environment in co-simulation with Matlab-Simulink® to show the controller’s performance against different types of disturbances. The results of a PID type controller are also contrasted with the results of the GPI controller.

**Keywords:** virtual prototype; upper extremities exoskeleton to rehabilitation; trajectories rehabilitation



**Citation:** Blanco-Ortega, A.; Vázquez-Sánchez, L.; Adam-Medina, M.; Colín-Ocampo, J.; Abúndez-Pliego, A.; Cortés-García, C.; García-Beltrán, C.D. A Robust Controller for Upper Limb Rehabilitation Exoskeleton. *Appl. Sci.* **2022**, *12*, 1178. <https://doi.org/10.3390/app12031178>

Academic Editor: Shin-Da Lee

Received: 21 October 2021

Accepted: 3 January 2022

Published: 23 January 2022

**Publisher’s Note:** MDPI stays neutral with regard to jurisdictional claims in published maps and institutional affiliations.



**Copyright:** © 2022 by the authors. Licensee MDPI, Basel, Switzerland. This article is an open access article distributed under the terms and conditions of the Creative Commons Attribution (CC BY) license (<https://creativecommons.org/licenses/by/4.0/>).

## 1. Introduction

Robotics can increase efficiency in the rehabilitation process of people who have suffered a stroke by using devices, such as exoskeletons, to provide continuous, smooth and controlled movements (position, speed, number of repetitions, among other factors) [1]. Stroke is the result of a shortage of blood supply to the brain that leads to cell death, causing severe damage to the human body, even death of the patient. Cardiovascular diseases and stroke produce immense health and economic costs in the United States and around the world. In the United States, stroke has become one of the leading causes of long-term severe disability [2,3], and is the second leading cause of disability worldwide [4]. Survivors who have suffered a stroke usually suffer from hemiparesis or total loss of movement. Stroke greatly affects the patient’s ability to perform tasks and activities of daily life. Therefore, it is vital to start a rehabilitation process to prevent spasticity, decreased muscle tone, increased stiffness, and loss of extensibility. In the rehabilitation process, patients can strengthen their weakened muscles, regain their range of motions, and thus restore their motor functions gradually [5].

Robotic devices, such as exoskeletons, have been proposed for incorporation into physical therapy. An exoskeleton is a mechanical structure designed to be used on the human body (structure similar to that of a human) as a garment, and both serves as a support and is used to assist movements or increase strength in a human [3,6,7]. Exoskeletons have been developed for lower, upper or full limbs (both extremities). These devices can contribute to passive, active and resistive rehabilitation. In passive rehabilitation, the patient receives the movements from the exoskeleton (active exoskeleton–passive patient); in the active, the patient provides the movements (passive exoskeleton–active patient); in the resistive, the exoskeleton opposes the user’s movement. In the control for a passive rehabilitation, strategies are used for trajectory tracking, since the exoskeleton is what will gently move the patient’s limb.

Some recently reported exoskeletons for upper extremity rehabilitation are listed below.

The 6-REXOS is a 6-DOF (degrees of freedom) exoskeleton that provides the movements of: elbow flexion–extension, forearm supination–pronation, flexion–extension and radial–ulnar deviation of the wrist. It has four active rotational and two passive translational junctions to allow kinematic redundancy to the exoskeleton [8,9]. MIT-Manus provides a robot-assisted therapy: a person sitting at a table puts the lower arm and wrist into a brace attached to the arm of the robot. A video screen prompts the person to perform an arm exercise such as connecting the dots. If movement does not occur, MIT-Manus moves the person's arm. If the person begins to move by themselves, the robot provides adjustable levels of guidance and assistance to facilitate the movement of the person's arm [10].

A shoulder exoskeleton of 6 DOF (two active and four passive) [11] has been developed that is composed of two spherical mechanisms, two sliding crank mechanisms, and a gravity compensation method. The exoskeleton uses linear series elastic actuators to implement impedance control at the exoskeleton–limb interface. Another example is a 5-DOF exoskeleton [12]; the shoulder was modeled as a 4-DOF joint by adding the shoulder elevation as a vertical movement, and the elbow was modeled as one DOF hinge joint. The authors performed direct and inverse kinematic analysis to verify that the proposed system was capable of reaching all points in the workspace.

Cost is a design factor to consider, so a low cost robot has been proposed for upper extremity rehabilitation [13]; this robot has a mechanism to compensate for the effect of gravity so that the patient does not feel the weight of the robot. By changing the direction of the actuator in relation to the user, the robot can provide flexion/extension, abduction/adduction, horizontal abduction/adduction, internal/external rotation, and oblique lifting movements.

Most shoulder rehabilitation devices are structures that are fixed to the ground and are not portable like exoskeletons. Table 1 presents a summary of some upper extremity rehabilitation devices.

In this paper, a 3-DOF upper extremity robot configuration is proposed. With these DOF, the movements of flexion–extension and abduction–adduction of the arm and flexion–extension of the forearm can be provided (Figure 1). In patients with hemiplegia, the objective of the controller is to allow the rehabilitator to provide smooth movements that follow a desired trajectory for passive rehabilitation. To achieve this, the use of a robust generalized proportional integral (GPI) controller is proposed for trajectory tracking, which is compared with a PID type controller. Furthermore, the proposed exoskeleton being portable will allow people who are located far from rehabilitation centers to access one and receive the appropriate therapy; this will avoid discomfort and costs in additional transfers.

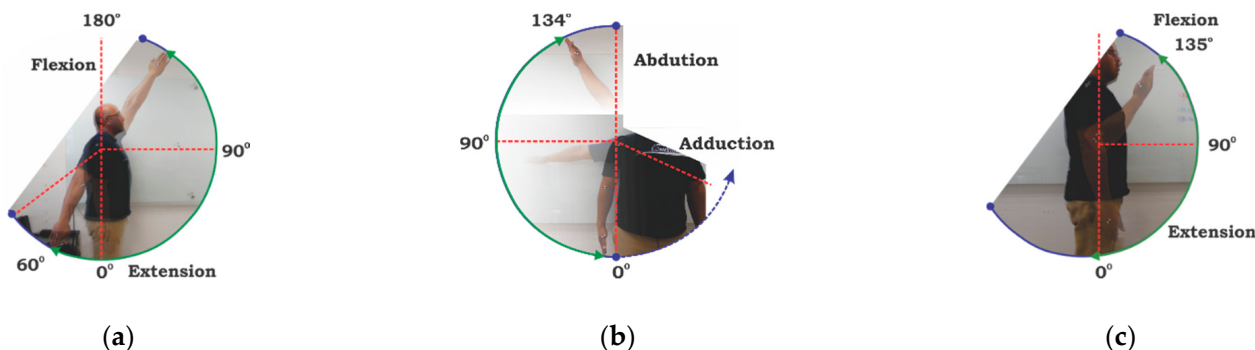


**Figure 1.** Movements of: (a) flexion–extension; (b) abduction–adduction of the arm (from that angle approximately, an additional DOF is made to reach 180°); (c) flexion–extension of the forearm.

**Table 1.** Upper limb exoskeletons for rehabilitation and assistance.

Reference	DOF	Actuator	Purpose and Movement Mode	Movements	Control	Portable
Krebs et al., 2004 [10]	7-different modules	DC motors	Stroke rehabilitation	Wrist, shoulder, arm	Force	N
Rosales et al., 2018 [14]	5	n.a.	Shoulder rehabilitation	F-E, AB-AD, internal/external rotation	Adaptive sliding modes	Y
Destarac et al., 2018 [15]	5	Servomotor DC	Rehabilitation	Shoulder: F-E, internal/external rotation, AB-AD Elbow: F-E	Without control	N
Onozuka et al., 2018 [16]	4	Magnetorheological clutches and artificial muscles	Assistance (elastic force)	Shoulder: AB-AD, F-E, internal/external rotation Elbow: F-E	Force feedback device	N
Su et al., 2018 [17]	5	Stepper motors	Rehabilitation	Elbow: F-E Forearm: P-S, Wrist: R-U, F-E, circumduction	Open loop control	Y
Ugurlu et al., 2015 [18]	6	AC brushless servo motors	Rehabilitation and power assistance tasks	Shoulder: F-E, internal/external rotation, Elbow: F-E	Impedance control	Y
Brahmi et al., 2018 [19]	7	Brushless DC motors	Motion Assistive	Shoulder: AB-AD, F-E, P-S, internal/external rotation Elbow: F-E Wrist: R-U, F-E	Adaptive backstepping control	N
Abooe et al., 2018 [20]	5	AC and DC servo motors	Rehabilitation	Shoulder: AB-AD, F-E, internal/external rotation; Elbow: F-E Wrist: F-E	Nonsingular terminal sliding mode control	N
Crocher et al., 2018 [21]	4	DC motors	Neurological rehabilitation	Shoulder: AB-AD, F-E, internal/external rotation	Compliance and impedance control	N

F-E = flexion/extension; C = circumduction = C; P-S = pronation/supination; AB-AD = abduction/adduction; R-U = radial/ulnar; n/a = not available.

## 2. Development

Figure 2a shows the exoskeleton for rehabilitation of the right upper extremity, indicating its main components. The exoskeleton is designed to place the motors in the base that is placed on the back of the user. The movement of the links of the arm and forearm will be made through cables connected to the motors. However, in this analysis, it is considered that the torques act directly on the shoulder and elbow joints in order to estimate the torque required in the engines when using cables. The three degrees of freedom to provide the movements of flexion–extension and abduction–adduction of the arm and flexion–extension of the forearm are shown in Figure 2b.

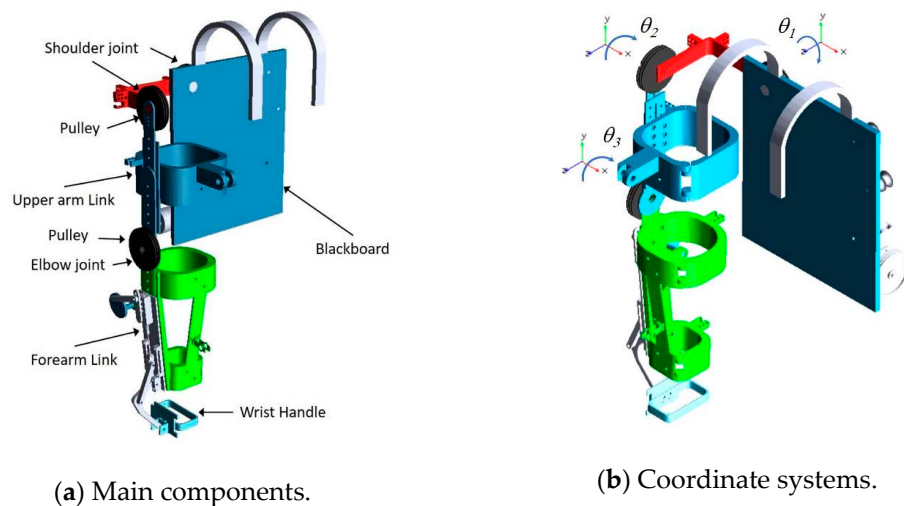


**Figure 2.** CAD view showing the architecture of the 3-DOF upper limb rehabilitation exoskeleton.

To achieve the objective of the controller that tracks the trajectory of the exoskeleton links, a proportional-integral robust controller (GPI) based on integral reconstructs for time-dependent first-order disturbances was designed. The procedure for the controller design is the same for each of the three actuators, so the development of the controller is shown in a general way.

The mechanical part of the exoskeleton arm has a weight of 2.51 kg, and the base where the motors are placed with all the components for their operation is 6 kg, which makes the exoskeleton light. The materials used were aluminum and Nylamid; some parts were machined in steel. The approximate weight of the exoskeleton is 8.5 kg. Although adding weight to a person who has suffered an injury may generate another injury of lower intensity, it should be understood that sometimes such sacrifices are necessary.

In relation to Table 1, most designs have 5 DOF, and the movements are almost coincidental. In the same way, the application is mostly focused on rehabilitation, with most of the authors focusing on stroke rehabilitation. Our design has a substantial relationship to the rehabilitation of stroke. We decided on 3 DOF because rehabilitation experts indicate that to regenerate the neuronal bonds of the damaged brain, it is appropriate to use the basic DOF, since saturating the brain with information can, depending on the damage caused, cause more posttraumatic stress.

Robot-mediated therapy has been found to produce improvements in the recovery of motor capacity; however, so far, the use of robots has not shown qualitative benefit over classical therapist-led training sessions performed on the same quantity of movements. Multi-degree-of-freedom robots, like the modern upper-limb exoskeletons, enable distributed interactions across the whole assisted limb, and can exploit a large amount of sensory feedback data, potentially providing new capabilities within standard rehabilitation sessions. Surprisingly, most publications in the field of exoskeletons have focused only on mechatronic device designs, while little focus has been given to the control aspects. On the contrary, a primordial aspect for the potentiality of robots resides in the control part [3].

Portable exoskeleton designs address the problem of the weight thereof, and this situation involves placing motors (ASME-03B High Power High Voltage Servo Motor 12 V ~ 24 V 380 kg/m 0.5 s/60°) in the middle of the back. Transmission pairs are with Bowden cables, and pulley arrangement is used to minimize torque. The arrangement of pulleys and motors does not need to be aligned.

Rosales, 2018 used several controllers: PD, PID, PD + g Adapt, and the adaptive sliding mode (Slide), and these were simulated in the dynamic model. Regulation tests were performed to compare the different controllers that were proposed, and graphs only giving position results with respect to time were shown. The torque required to dimension the motor suitable for use in the design was nonspecific. In the case of exoskeletons,

Destarac, 2018 did not use a control technique, but information was generated for design development and testing in order to characterize DOF.

Onozuka, 2018 presented a different type of exoskeleton, accompanied by different kinds of actuators, in relation to most existing exoskeletons, both in research and in the world market, as this proposed exoskeleton tries to emulate a muscle. The forces required for each DOF between the displacement and load were specified. The control system for the forced feedback device takes into account the stiffness and the torque required for each shift. Additionally, in applying the methodology proposed, weight reduction to a manipulator that controls only the outside, not the moments, takes place, which is also the case in Crocher, 2018.

### 3. Controller for Trajectory Tracking

Model-based controllers are not easy to implement and cannot provide precise control in the human–exoskeleton interaction, because exoskeleton–human interaction factors and sensor noise do not allow the exact dynamic model to be taken into account. Therefore, several systems are controlled independently in the active joints [22,23].

Effective rehabilitation exercises require precise, stable and reliable control techniques. The traditional PID controller is commonly used due to its good features, such as its robustness, simplicity and wide applicability [24].

#### 3.1. PID Type Control with Trajectory Tracking

To achieve the desired control response, only active joints are considered, and the following PID type controller is proposed.

$$\tau_i = J_e \left[ \ddot{q}_{id} - k_d(\dot{q}_i - \dot{q}_{id}) - k_p(q_i - q_{id}) - k_i \int (q_i - q_{id}) dt \right] \quad (1)$$

where  $J_e$  represents the equivalent moment of inertia of the link where the torque is applied with the other joined links in which it performs the movement. The desired trajectory is denoted by  $q_i$ ,  $\dot{q}_i$  and  $\ddot{q}_{id}$ . The proportional, integral and derivative gains of the controller are  $k_p$ ,  $k_i$  and  $k_d$ , respectively. By assigning poles, the controller's gains were determined, which remained as:

$$k_p = 212, k_i = 800, k_d = 12.$$

#### 3.2. Robust GPI Type Control with Trajectory Tracking

The mathematical model of the 3-DOF exoskeleton can be obtained through the Euler–Lagrange equation, and can be given by the following structure:

$$M(\theta) \ddot{\theta}(t) + C(\theta(t), \dot{\theta}(t)) \dot{\theta}(t) + G(\theta(t)) = \tau(t) \quad (2)$$

where  $\theta \in R^3$ ,  $M(\theta)$ ,  $C(\theta, \dot{\theta})$  and  $G(\theta)$ , are the positive-definite and symmetric inertia matrix, the Coriolis matrix and the vector of gravitational terms, respectively.

Multiplying by  $M^{-1}(\theta)$

$$\ddot{\theta}(t) = M^{-1}(\theta)\tau(t) - M^{-1}(\theta) \left[ C(\theta(t), \dot{\theta}(t)) \dot{\theta}(t) + G(\theta(t)) \right] \quad (3)$$

Consider

$$\begin{aligned} \xi(t) &= -M^{-1}(\theta) \left[ C(\theta(t), \dot{\theta}(t)) \dot{\theta}(t) + G(\theta(t)) \right] \\ u(t) &= M^{-1}(\theta)\tau(t) \end{aligned} \quad (4)$$

The dynamic model of the 3-DOF exoskeleton system can be represented as a disturbed system given by:

$$\ddot{\theta}_i(t) = u_i(t) + \xi_i(t) \quad (5)$$

Assuming that  $\xi_i(t)$  is unknown but uniformly bounded and absolute. The model results in a system of equations, so three independent control inputs can be defined for robust trajectory tracking:

$$u_i = \ddot{\theta}_{id} - k_3 \left( \widehat{\dot{\theta}}_i - \dot{\theta}_{id} \right) - k_2(\theta_i - \theta_{id}) - k_1 \int_0^t (\theta_i - \theta_{id}) d\tau - k_0 \int_0^t \int_0^\tau (\theta_i - \theta_{id}) d\lambda d\tau \quad (6)$$

where (5) is the integral reconstruction of the speed of the corresponding link.

$$\begin{aligned} \widehat{\dot{\theta}}_i &= \int_0^t u_i d\tau \\ \dot{\theta}_i &= \widehat{\dot{\theta}}_i + \dot{\theta}_{i0} \end{aligned} \quad (7)$$

Substituting (6) in (5), and considering the integral reconstruction (7) and the disturbance,

$$\begin{aligned} \ddot{\theta}_i &= \ddot{\theta}_{id} - k_3 \left( \widehat{\dot{\theta}}_i - \dot{\theta}_{id} \right) - k_2(\theta_i - \theta_{id}) - k_1 \int_0^t (\theta_i - \theta_{id}) d\tau \\ &\quad - k_0 \int_0^t \int_0^\tau (\theta_i - \theta_{id}) d\lambda d\tau + a_1 t + a_0 \end{aligned} \quad (8)$$

Defining the error as  $e = \theta_i - \theta_{id}$ , and deriving twice results in a dynamic equation of the error given by

$$e^{IV} + k_3 \ddot{e} + k_2 \dot{e} + k_1 e + k_0 e = 0 \quad (9)$$

Applying the Laplace transform to (9) with initial conditions equal to zero, the characteristic equation of the closed-loop system is obtained:

$$s^4 + k_3 s^3 + k_2 s^2 + k_1 s + k_0 = 0 \quad (10)$$

The controller gains ( $k_i$ ,  $i = 0, 1, 2, 3$ ) are determined by equating a Hurwitz polynomial so that the error dynamics are asymptotically stable.

$$(s^2 + 2\zeta_1 \omega_1 s + \omega_1^2)(s^2 + 2\zeta_2 \omega_2 s + \omega_2^2) = 0 \quad (11)$$

For this case, the following were selected:

$$\zeta_1 = \zeta_2 = 1.5 \text{ and } \omega_1 = \omega_2 = 8$$

Considering that the different parameters, such as the varying sizes, weights, and heights of humans that will use an exoskeleton for rehabilitation, will result in a dynamic modeling of a system with uncertainties, it is necessary to propose a control law that is robust. In the previous case, the controller considers a variant disturbance in the ramp type time; in this case, it is considered to be given by the following third degree polynomial:

$$\xi_1 = a_3 t^3 + a_2 t^2 + a_1 t + a_0 \quad (12)$$

To compensate for the disturbance and to achieve the controller's objective of tracking the desired trajectory, the following robust controller is proposed.

$$\begin{aligned} u_1 &= \ddot{z}_{1d} - k_5 \left( \dot{z}_1 - \dot{z}_{1d} \right) - k_4(z_1 - z_{1d}) - k_3 \int_0^t (z_1 - z_{1d}) d\tau - k_2 \int_0^t \int_0^\tau (z_1 - z_{1d}) d\lambda d\tau \\ &\quad - k_1 \int_0^t \int_0^\tau \int_0^\lambda (z_1 - z_{1d}) d\sigma d\lambda d\tau - k_0 \int_0^t \int_0^\tau \int_0^\lambda \int_0^\sigma (z_1 - z_{1d}) d\rho d\sigma d\lambda d\tau \end{aligned} \quad (13)$$

The use of the robust GPI controller (13) yields the following closed-loop dynamics for the trajectory tracking error,  $e(t) = z_1 - z_{1d}(t)$ :

$$e^{VI} + k_5 e^V + k_4 e^{IV} + k_3 \ddot{e} + k_2 \dot{e} + k_1 e + k_0 e = 0 \quad (14)$$

The characteristic equation of the system is now:

$$s^6 + k_5 s^5 + k_4 s^4 + k_3 s^3 + k_2 s^2 + k_1 s + k_0 = 0 \quad (15)$$

The parameters were selected to ensure that the error dynamics were globally asymptotically stable. This is carried out by a term by term equalization of the closed-loop characteristic polynomial with the desired polynomial, given by:

$$(s^2 + 2\zeta\omega s + \omega^2)^3 = 0 \quad (16)$$

where  $\zeta = 1.3$ ,  $\omega = 8$ .

The robust GPI controller (13) is depicted in block diagram (Figure 3). It can be seen that the controller only requires output measurements (link angle).

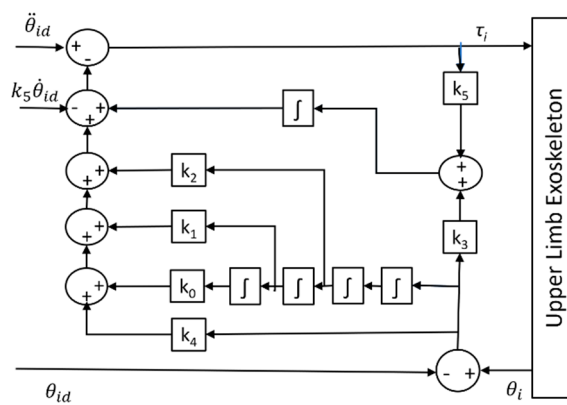


**Figure 3.** Block diagram of the robust GPI controller, considering the third-order polynomial perturbation.

### 3.3. Trajectory Desired

A Bézier polynomial interpolated between the initial position and the final position was used to follow the trajectory of the displacements of each link of the exoskeleton  $\theta_i$  [25].

The desired position path is given by the following Bézier polynomial:

$$\begin{aligned} \theta_{id} &= \theta_i + (\theta_{if} - \theta_{i0}) \sigma(t, t_{i0}, t_{if}) \mu_p^5 \\ \sigma(t, t_i, t_f) &= \gamma_1 - \gamma_2 \mu_p + \gamma_3 \mu_p^2 - \cdots + \gamma_6 \mu_p^5 \\ \mu_p &= \frac{t-t_i}{t_f-t_i} \end{aligned} \quad (17)$$

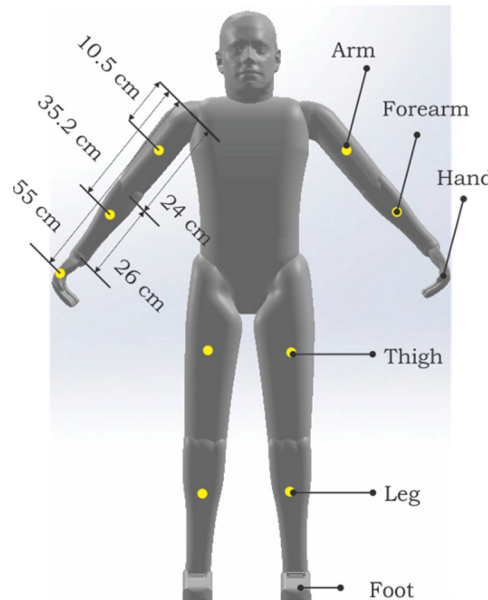
where  $\theta_{i0} = \theta_d(t_{i0})$  and  $\theta_{if} = \theta_d(t_{if})$  are the initial and final desired positions. The parameters of the polynomial function (9) are  $\gamma_1 = 252$ ,  $\gamma_2 = 1050$ ,  $\gamma_3 = 1800$ ,  $\gamma_4 = 1575$ ,  $\gamma_5 = 700$  and  $\gamma_6 = 126$ .

## 4. Simulation Results

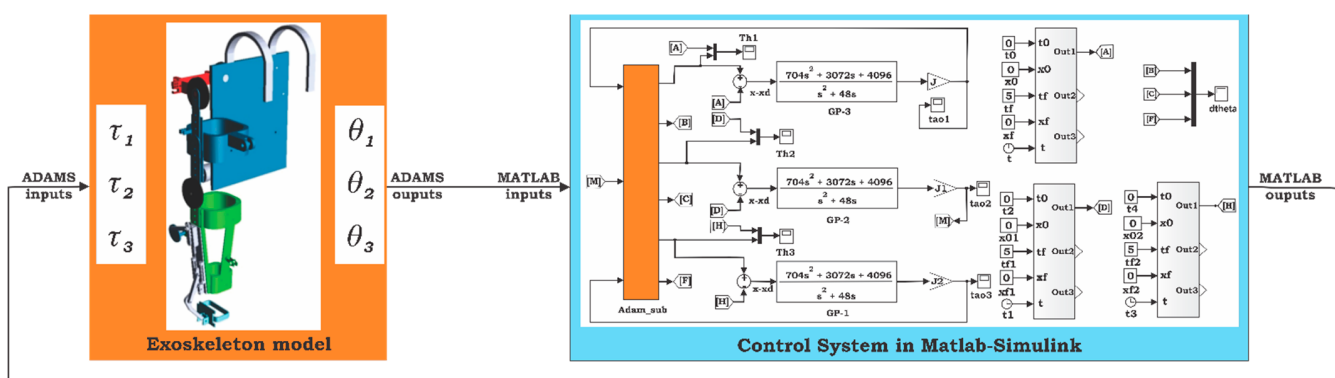
For the simulations, the anthropometric dimensions of the user in the exoskeleton were considered, as well as the forces that represent the weight of each segment of the limb. These simulations considered the weight of an average patient of 80 kg. Table 2 shows the center of mass length from the shoulder and the mass of each segment of the patient's arm. The length to the center of mass of the segments for the patient's arm, as well as for the segments for exoskeleton are shown in Figure 4. In this center of mass, the patient's weight is considered to act as a disturbance not known to the controller and one which always remains in the direction of gravity.

**Table 2.** Length and mass values of the upper limb segments.

Segments	Mass (kg)	Center of Mass Length from Shoulder (cm)
Arm	2.2	10.5
Forearm	1.3	35.2
Hand	0.5	55

**Figure 4.** Length and center-of-mass location of the upper limb segments.

The simulation results were obtained by implementing the robust GPI controller in the virtual prototype, under the MSC Adams view® software environment, and in co-simulation with Matlab-Simulink® (Figure 5). From the virtual prototype, the signals of the exoskeleton link angles were sent to Matlab-Simulink®; in this software, the calculation of the robust GPI controller is carried out by tracking the desired trajectory, and the control input (torques) is sent to the virtual prototype.

**Figure 5.** Block diagram in Simulink of robust GPI control in co-simulation with MSC Adams view®.

Two views of the virtual prototype of the exoskeleton are shown under the MSC Adams® software environment (Figure 6). In these, the forces that represent the weight of each segment of the patient's arm can be appreciated. These forces enter as disturbances unknown to the controller and always act in the direction of gravity. The controller was given an approximate value of inertia  $M(\theta)$  (see Equation (4)), so there are also parametric uncertainties that the robust GPI controller compensates for. It is also shown that the

controller is robust in the uncertainty of the gain of the controller, which represents the inertia of the system (link) [26].

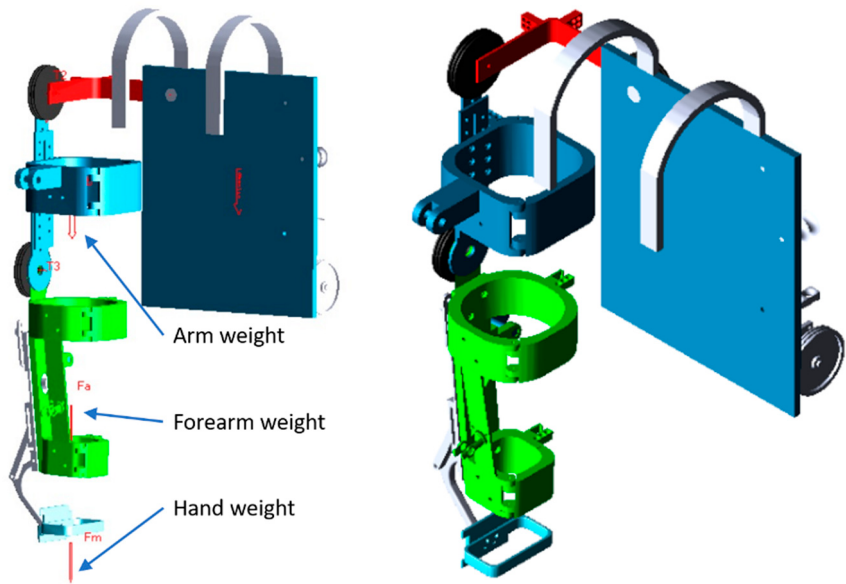


**Figure 6.** CAD view showing the architecture of the 3-DOF upper limb rehabilitation exoskeleton considering segment weights.

#### 4.1. Results with the PID Type Controller

The exoskeleton response with the PID controller (4) with trajectory tracking to achieve a  $90^\circ$  bending movement in 5 s is shown in Figure 7. The Bézier polynomial Equation (17) was used to achieve a smooth movement, as shown for the angle  $\theta_2$ . It is important to mention that in this simulation, the weight derived from the limb of the patient to be rehabilitated was not considered, only the inertia of the links. It is observed that there is a control effort in all the links to keep the exoskeleton in a flexed position.

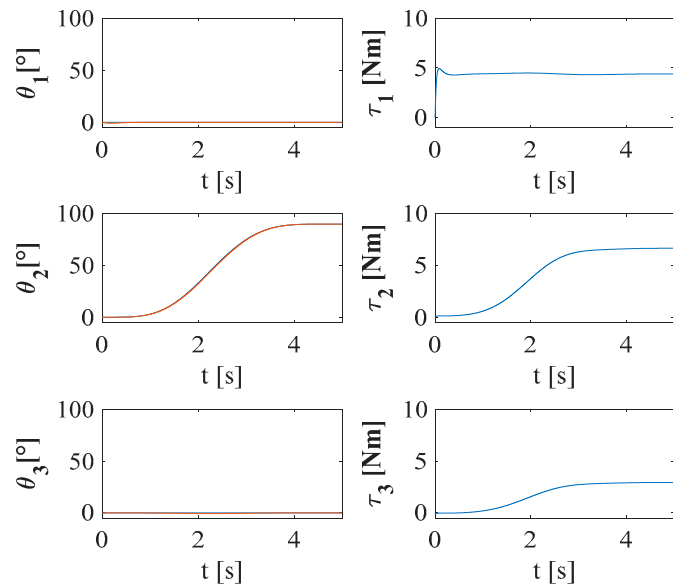


**Figure 7.** Response for a flexion movement without considering the weight of the patient's arm.

Figure 8 shows the response of the exoskeleton with the PID controller with trajectory tracking to achieve a  $90^\circ$  bending movement in 5 s. In this simulation, the weight derived from the limb of the patient to be rehabilitated was considered, as shown in Figure 6. It

can be seen that trajectory tracking is adequate, considering the strength derived from the weight of the user's arm and the parametric uncertainties. Although there were some deviations in the angles of  $\theta_1$  and  $\theta_3$ , these were less than 2 degrees, which may be imperceptible to the user, since it is not a sudden variation (sudden movement).

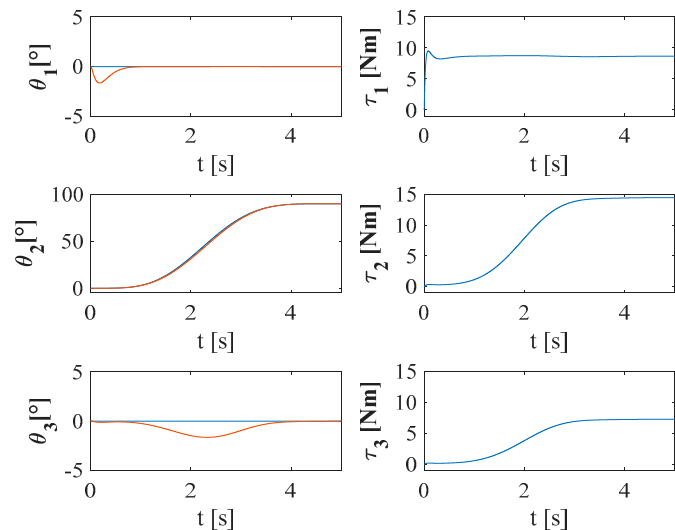


**Figure 8.** Response for a flexion movement with the PID controller considering the weight of the patient's arm.

#### 4.2. Results with the Robust GPI Controller

The response of the exoskeleton with the robust GPI controller (6) with trajectory tracking to achieve a  $90^\circ$  bending movement in 5 s is shown in Figure 9. The Bézier polynomial was used to achieve a smooth movement, as shown for the angle  $\theta_2$ . In this simulation, the weight derived from the limb of the patient to be rehabilitated was considered. Compared with the response using the PID type controller, it is observed that this response follows the desired trajectory without increasing the control effort. The advantage of this controller is that it only requires knowledge of the output (angular position), reducing cost and data processing.

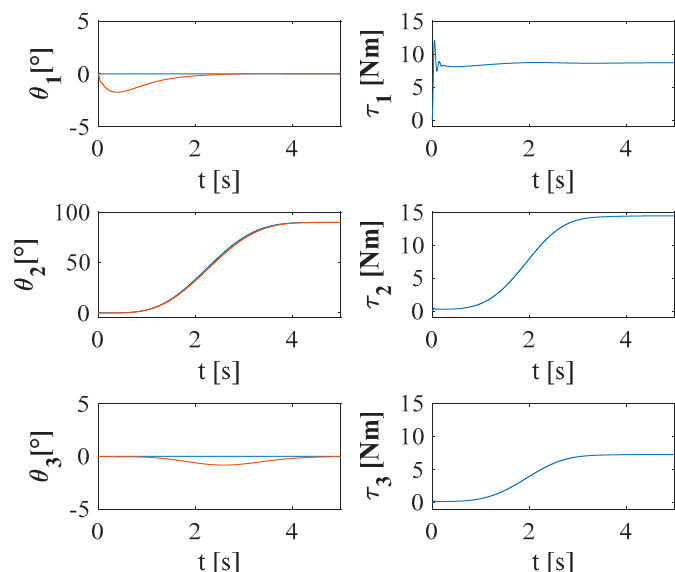


**Figure 9.** Response for a flexion movement with the GPI controller, given by Equation (6), considering the weight of the patient's arm.

The response of the exoskeleton with the robust GPI controller (13) with trajectory tracking to achieve a  $90^\circ$  bending movement in 5 s is shown in Figure 10. In this simulation, the weight derived from the limb of the patient to be rehabilitated was also considered. As shown in the results, it achieved a better performance, minimizing the error and still maintaining a control effort similar to the PID controller (1) and the robust controller GPI (6) for ramp-type disturbances.

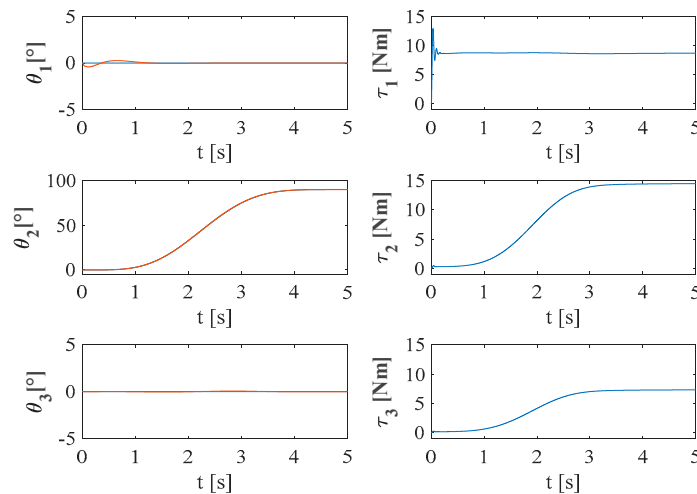


**Figure 10.** Response for a flexion movement with the GPI controller, given by Equation (13), considering the weight of the patient's arm.

Next, the exoskeleton response is shown for abduction movement ( $45^\circ$ ) and flexion ( $45^\circ$ ) of the arm, and for flexion ( $90^\circ$ ) of the forearm (Figure 11), considering the masses of the arm (Table 2) as forces acting on the exoskeleton (Figure 12). The GPI controller (13) was used with the trajectory tracking defined by the Bézier polynomial (17). The movements were performed at the same time, for 5 s, to reach the desired value. It can be seen that the controller achieved a good performance in tracking the trajectory, and the control effort of all links was kept below 15 Nm when performing the combined movements. Figure 12 shows the exoskeleton in the desired final position considering the combined movements.

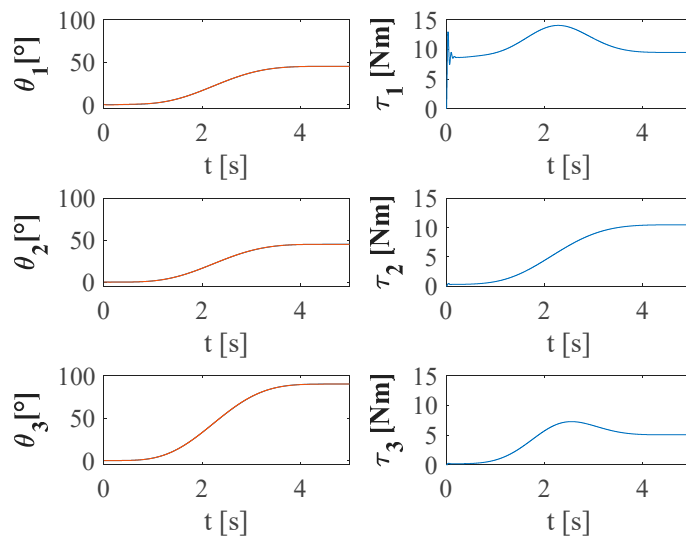


**Figure 11.** Response for a combined movement with the GPI controller, given by Equation (13), considering the weight of the patient's arm.

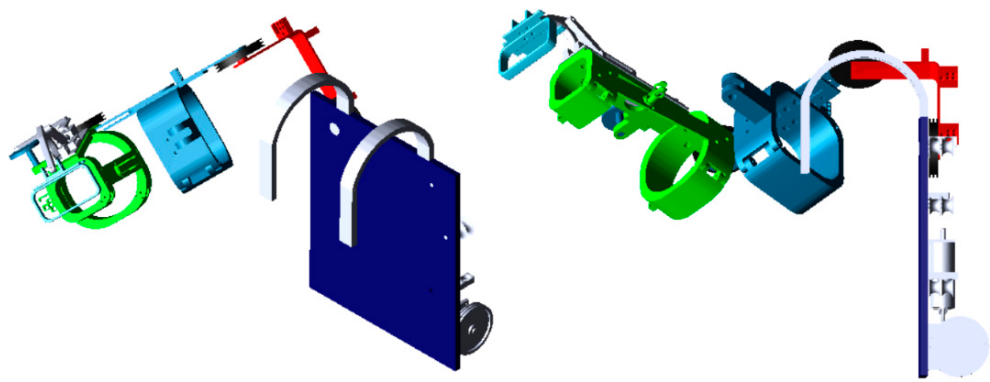


**Figure 12.** CAD view showing the upper limb rehabilitation exoskeleton.

Muscle spasticity was quantified by muscle displacements and compliance of myotonometer measurements and resistive torques from repeated passive stretching at speeds of  $5 \frac{\circ}{s}$  and  $10 \frac{\circ}{s}$ , where stiffness ( $0.17 \text{ Nm}/\circ$ ) total muscle was estimated, and muscle spasticity was analyzed in chronic stroke survivors using myotonometry and conventional passive stretching techniques [27]. The elbow flexor torque  $\tau_s$  is a function of forearm flexion  $\theta_3$ .

The control of the combined motion of the exoskeleton was performed using a GPI control (13), with trajectory tracking defined by the Bézier polynomial (17), for the abduction ( $45^\circ$ ) and flexion ( $45^\circ$ ) motions of the arm and the flexion ( $90^\circ$ ) of the forearm (Figure 13), also considering the arm masses held in Table 2 and the forces acting on the exoskeleton and the elbow flexor torque  $\tau_s$ . The movements were performed at the same time, for 5 s, to reach the desired value. It is observed that the controller achieved a good performance in trajectory tracking, and only the control effort in the second link ( $\tau_2$ ) increased to 26 Nm (Figure 13) when performing the combined movements to compensate for the elbow flexor torque (Figure 14).

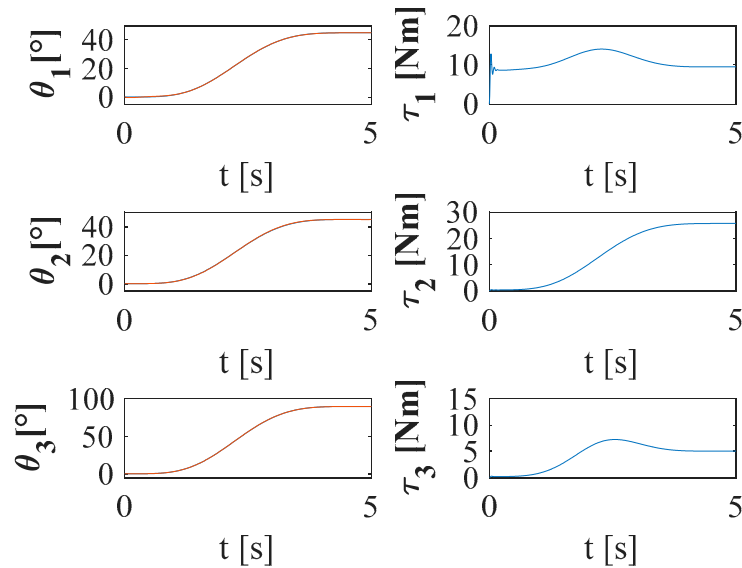


**Figure 13.** Response for a combined movement with the GPI controller, given by Equation (13), considering the weight of the patient's arm and elbow flexor torque (spasticity).

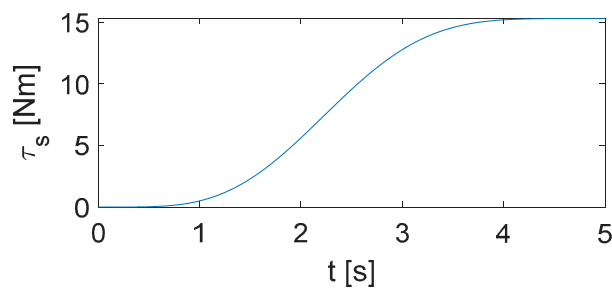


**Figure 14.** Elbow flexor torque ( $0.17 \text{ Nm/}^\circ$ ) in function of  $\theta_3$ .

## 5. Conclusions

The exoskeletons have shown that they can contribute to a better rehabilitation process by improving movements and increasing the rehabilitation time and the number of sessions. To achieve a good performance requires controllers that are robust to disturbances (endogenous and exogenous) that can occur in the system.

In this paper, a robust GPI controller is proposed, which only requires output measurements (angular position of the link) for tracking desired trajectories. The simulation results show a good performance of the GPI controller with respect to the PID controller, with these results being obtained in the MSC Adams® software in co-simulation with Matlab-Simulink®.

In reference to the development of the exoskeleton for the rehabilitation of upper limbs, (a) it has to perform passive movements without reaching extremes that can generate excessive loads of muscle or joint stretching; the degrees of freedom that were designed will initially allow an active reach for limb stretching in order to regain movement and motor control; (b) it is safe, as the movement is assisted, and it has designed mechanical limits to avoid unwanted singularities; (c) portability is essential in this design, since in many cases receiving specialized assistance is complex due to the country or region where patients are located; (d) the cost of acquiring an exoskeleton is high.

There are various limitations, or rather there are challenges to be covered as the design, tests, mechanisms, etc., progresses, because emulating the movements of the upper extremities is very complex. It is not possible to cover all the movements carried out by an upper limb individually in real time and, if the movements carried out in combination with both upper limbs are annexed, the degrees of freedom increase, but exponentially with increases in the difficulty of adding mechanical, electrical and electronic components to the design. This only adds to the weight, and would make the exoskeleton no longer portable. The higher the portability, the fewer the degrees of freedom that can be added by the aforementioned.

In future work, the exoskeleton will be conditioned and instrumented to help patients to perform voluntary movements, and not only the previously programmed movements.

**Author Contributions:** A.B.-O. worked in the conceptualization, validation, simulations and control; L.V.-S. worked in the simulations, design and control, and wrote the initial manuscript; M.A.-M. and C.C.-G. worked in the conceptualization and performed the experiments; J.C.-O. and A.A.-P. worked on mechanical design; C.D.G.-B. worked on electrical design and control. All of the above authors analyzed the results and revised the paper. All authors have read and agreed to the published version of the manuscript.

**Funding:** This research received no external funding.

**Institutional Review Board Statement:** Not applicable.

**Informed Consent Statement:** Not applicable.

**Data Availability Statement:** Not applicable.

**Conflicts of Interest:** The authors declare no conflict of interest.

## References

1. Luna, C.O.; Rahman, M.H.; Saad, M.; Archambault, P.S.; Ferrer, S.B. Admittance-Based Upper Limb Robotic Active and Active-Assistive Movements. *Int. J. Adv. Robot. Syst.* **2015**, *12*, 117. [[CrossRef](#)]
2. Benjamin, E.; Blaha, M.; Chiave, S. Heart disease and stroke statistics—2017 update: A report from the American heart association. *Circulation* **2017**, *131*, 146–603. [[CrossRef](#)] [[PubMed](#)]
3. Rehmat, N.; Zuo, J.; Meng, W.; Liu, Q.; Xie, Q.; Liang, H. Upper limb rehabilitation using robotic exoskeleton systems: A systematic review. *Int. J. Intell. Robot. Appl.* **2018**, *2*, 283–295. [[CrossRef](#)]
4. Stewart, A.M.; Pretty, C.G.; Adams, M.; Chen, X. Review of Upper Limb Hybrid Exoskeletons. *IFAC-PapersOnLine* **2017**, *50*, 15169–15178. [[CrossRef](#)]
5. Li, J.; Zhang, Z.; Tao, C.; Ji, R. A number synthesis method of the self-adapting upper-limb rehabilitation exoskeletons. *Int. J. Adv. Robot. Syst.* **2017**, *14*, 1729881417710796. [[CrossRef](#)]
6. Lee, H.-D.; Lee, B.-K.; Kim, W.-S.; Han, J.-S.; Shin, K.-S.; Han, C.-S. Human–robot cooperation control based on a dynamic model of an upper limb exoskeleton for human power amplification. *Mechatronics* **2014**, *24*, 168–176. [[CrossRef](#)]
7. Marcheschi, S.; Salsedo, F.; Fontana, M.; Bergamasco, M. Body Extender: Whole body exoskeleton for human power augmentation. *IEEE Int. Conf. Robot. Autom.* **2011**, *9*, 611–616. [[CrossRef](#)]
8. Gunasekara, M.; Gopura, R.; Jayawardena, S. 6-REXOS: Upper Limb Exoskeleton Robot with Improved pHRI. *Int. J. Adv. Robot. Syst.* **2015**, *12*, 47. [[CrossRef](#)]
9. Gopura, R.; Bandara, D.; Kiguchi, K.; Mann, G. Developments in hardware systems of active upper-limb exoskeleton robots: A review. *Robot. Auton. Syst.* **2016**, *75*, 203–220. [[CrossRef](#)]
10. Krebs, H.I.; Ferraro, M.; Buerger, S.P.; Newberry, M.J.; Makiyama, A.; Sandmann, M.; Lynch, D.; Volpe, B.T.; Hogan, N. Rehabilitation robotics: Pilot trial of a spatial extension for MIT-Manus. *J. NeuroEng. Rehabil.* **2004**, *1*, 5. [[CrossRef](#)]
11. Hsieh, H.-C.; Chen, D.-F.; Chien, L.; Lan, C.-C. Design of a Parallel Actuated Exoskeleton for Adaptive and Safe Robotic Shoulder Rehabilitation. *IEEE/ASME Trans. Mechatron.* **2017**, *22*, 2034–2045. [[CrossRef](#)]
12. Jung, Y.; Bae, J. Kinematic Analysis of a 5-DOF Upper-Limb Exoskeleton with a Tilted and Vertically Translating Shoulder Joint. *IEEE/ASME Trans. Mechatron.* **2015**, *20*, 1428–1439. [[CrossRef](#)]
13. Lee, K.-S.; Park, J.-H.; Park, H.-S. Compact design of a robotic device for shoulder rehabilitation. In Proceedings of the 2017 14th International Conference on Ubiquitous Robots and Ambient Intelligence (URAI), Jeju, Korea, 28 June–1 July 2017; pp. 679–682. [[CrossRef](#)]
14. Rosales, L.; Lopez-Gutierrez, R.; Salazar, S.; Lozano, R. Robust controls for upper limb exoskeleton, real-time results. *Proc. Inst. Mech. Eng. Part I J. Syst. Control. Eng.* **2018**, *232*, 797–806. [[CrossRef](#)]
15. Destarac, M.A.; Cena, C.E.G.; García, J.; Espinoza, R.; Saltaren, R.J. ORTE: Robot for Upper Limb Rehabilitation. Biomechanical Analysis of Human Movements. *IEEE Lat. Am. Trans.* **2018**, *16*, 1638–1643. [[CrossRef](#)]
16. Onozuka, Y.; Suzuki, R.; Yamada, Y.; Nakamura, T. An Exoskeleton Type 4-DOF Force Feedback Device Using Magnetorheological Fluid Clutches and Artificial Muscles. In Proceedings of the IEEE/ASME International Conference on Advanced Intelligent Mechatronics (AIM), Auckland, New Zealand, 9–1 July 2018; pp. 869–874. [[CrossRef](#)]
17. Su, Y.-Y.; Wu, K.-Y.; Lin, C.-H.; Yu, Y.-L.; Lan, C.-C. Design of a Lightweight Forearm Exoskeleton for Fine-Motion Rehabilitation. In Proceedings of the IEEE/ASME International Conference on Advanced Intelligent Mechatronics (AIM), Auckland, New Zealand, 9–12 July 2018; pp. 438–443. [[CrossRef](#)]
18. Ugurlu, B.; Nishimura, M.; Hyodo, K.; Kawanishi, M.; Narikiyo, T. Proof of Concept for Robot-Aided Upper Limb Rehabilitation Using Disturbance Observers. *IEEE Trans. Hum.-Mach. Syst.* **2014**, *45*, 110–118. [[CrossRef](#)]
19. Brahmi, B.; Saad, M.; Ochoa-Luna, C.; Rahman, M.; Brahmi, A. Adaptive Tracking Control of an Exoskeleton Robot with Uncertain Dynamics Based on Estimated Time-Delay Control. *IEEE/ASME Trans. Mechatron.* **2018**, *23*, 575–585. [[CrossRef](#)]
20. Abooe, A.; Arefi, M.M.; Sedghi, F.; Abootalebi, V. Robust nonlinear control schemes for finite-time tracking objective of a 5-DOF robotic exoskeleton. *Int. J. Control.* **2019**, *92*, 2178–2193. [[CrossRef](#)]
21. Crocher, V.; Fong, J.; Bosch, T.J.; Tan, Y.; Mareels, I.; Oetomo, D. Upper Limb Deweighting Using Underactuated End-Effector-Based Backdrivable Manipulanda. *IEEE Robot. Autom. Lett.* **2018**, *3*, 2116–2122. [[CrossRef](#)]
22. Chen, K.-Z.; Song, Q.-Z.; Wang, X.-G.; Wang, X. Joint Control of the Upper Limb Exoskeleton Based on Fuzzy-PD. *DEStech Trans. Comput. Sci. Eng.* **2017**. [[CrossRef](#)]
23. Sira-Ramírez, H.; Beltran-Carbajal, F.; Blanco-Ortega, A. A generalized proportional integral output feedback controller for the robust perturbation rejection in a mechanical system. *STA* **2008**, *5*, 24–32.
24. Rahman, M.; Saad, M.; Ochoa-Luna, C.; Kenne, J.; Archambault, P. Cartesian Trajectory Tracking of an Upper Limb Exoskeleton Robot. In Proceedings of the IECON 2012–38th Annual Conference on IEEE Industrial Electronics Society, Montreal, QC, Canada, 25–28 October 2012; pp. 2668–2673. [[CrossRef](#)]
25. Klopčar, N.; Lenarčič, J. Kinematic Model for Determination of Human Arm Reachable Workspace. *Meccanica* **2005**, *40*, 203–219. [[CrossRef](#)]
26. Athar, A.; Syed, F.; Kushsairy, A.; Kamran, M.; Yaroq, S. Fuzzy PID controller for upper limb rehabilitation robotic system. In Proceedings of the IEEE International Conference on Innovative Research and Development (ICIRD), Bangkok, Thailand, 11–12 May 2018; pp. 1–5. [[CrossRef](#)]
27. Li, X.; Shin, H.; Li, S.; Zhou, P. Assessing muscle spasticity with Myotonometric and passive stretch measurements: Validity of the Myotonometer. *Sci. Rep.* **2017**, *7*, srep44022. [[CrossRef](#)] [[PubMed](#)]